J Nanostruct 13(4): 1104-1114, Autumn 2023

RESEARCH PAPER

Inhibitory Effect of Iron and Zinc Oxides Core-Shell Nanoparticles Against Clinical Isolate of *Pseudomonas Aeruginosa*

Bakr Abdalatef Ahmed *, Laith Ahmed Yaaqoob

Department of Biotech, College. Science, University of Baghdad, Iraq

ARTICLE INFO

Article History:
Received 04 July 2023
Accepted 23 September 2023
Published 01 October 2023

Keywords:
Core-shell
Fe_2O_3:ZnO NPs
Prodigiosin
Pseudomonas aeruginosa
Serratia marcescenss

ABSTRACT

This study aimed to use Prodigiosin pigment produced by the environmental bacteria Serratia marcescensas as a reducing and stabilizing agent for core-shell nanoparticles of iron and zinc (Fe_2O_3:ZnO) and use it as antibacterial effectiveness against biofilm-forming, multidrug-resistant of pathogenic bacteria Pseudomonas aureginosa which was obtained from burn and wound. (Fe_2O_3:ZnO) NPs The preparation was in two phases, The first stage is the preparation of iron nanoparticles by adding (5g) of prodigiosin powder with (50ml) deionized distilled water DDW and add (5g) of ferric sulfate in (50ml) of prodigiosin pigment, In second phase add (1.5g) of iron nanoparticles in (150ml) of prodigiosin pigment and add (5g) of zinc acetate and shake it overnight in a darkroom at room temperature. The mixture was then centrifuged for 10 minutes at 5000 rpm. The precipitate of a solution containing the whole iron and zinc (Fe_2O_3:ZnO) core-shell nanoparticles. The (Fe_2O_3:ZnO)NPs biosynthesized were characterized by various techniques such as UV-VIS, AFM, , FTIR, FE-SEM,. based on the wavelength of the iron and zinc (Fe_2O_3:ZnO) core-shell nanoparticles at (284 nm) by spectrophotometer, The diameter was identified by Atomic force microscopy (AFM) the average diameter at 81.32nm, and the higher concentration of (Fe_2O_3:ZnO) NPS in the solution at 200 µg/ml It was shown that the maximum inhibitory zones for Pseudomonas aureginosa were 27 millimeters in diameter.

How to cite this article
Ahmed B., Yaaqoob L. Inhibitory Effect of Iron and Zinc Oxides Core-Shell Nanoparticles Against Clinical Isolate of Pseudomonas Aeruginosa. J Nanostruct, 2023; 13(4):1104-1114. DOI: 10.22052/JNS.2023.04.018

INTRODUCTION

The earliest forms of life, bacteria have the remarkable ability to change and evolve in response to their surroundings. Infectious illnesses caused by pathogenic microbes have been a major cause of human mortality throughout recorded history. Significant respite against infectious illnesses was provided by the finding of antimicrobial agents such as penicillin, macrolides, chloramphenicol, nalidixic acid and salvarsan in the early decades of the 20th century [1-3]. Due to the insufficient use of traditional antibiotics over a lengthy period of time, bacteria have evolved defenses that allow them to escape treatment [4-6]. As a result, there is an immediate need to investigate alternative methods for achieving effective bacterial identification and detection therapy [7-8].

One of these alternative methods is metal nanoparticles, which are particles with diameter of less than or equal to 100 nm and a high surface-to-volume ratio [9], and enhanced characteristics, including an altered particle size distribution and

* *Corresponding Author Email: bakrabdalatefahmedaljanabi@gmail.com*

shape. Its high value is attributable to the fact that changes in particular surface area have an effect on critical factors like surface reactivity [10-11].

In this context, Nanomaterials are the most promising and practical choice in fighting against bacterial diseases due to their membrane permeability, high biocompatibility, specific bactericidal processes, and extraordinary physicochemical features [12]. Inorganic nanoparticles are able to prevent bacteria from becoming resistant to them by causing toxins through multiple, non-specific processes. This expands the range of their bactericidal activity [13-15]. Studies on the effectiveness of metal nanoparticles such as Rh, Mn, Cu, Se, Pd, Au, Ag and metal oxide nanoparticles such as CuO, TiO_2 and ZnO, against Gram-positive and Gram-negative bacteria have been documented lately [10]. Other metal oxides, such as cerium oxide and manganese oxide, may also have antimicrobial qualities, though this is less well documented [16].

Nanoparticles with core-shell structures have attracted a lot of attention recently due to their unusual chemical and physical characteristics and wide range of possible uses. These heterostructured core-shell systems may exhibit traits of both the core and the shell, as well as additional functions and unusual exchange-couple characteristics [5,13]. Hence, this combination between nanoparticles which loaded into prodigiosin pigment improve their roles in inhibitory effects against pathogenic bacteria. An alkaloid secondary metabolite, called Prodigiosin, which produced by several organisms, including *Serratia marcescens*, *Pseudomonas magneslorubra*, *S. rubidaea*. This pigment characterized by several properties, such as antitumor activity, anticancer activity, antibacterial and antifungal activities [17]. One of these organisms that produce prodigiosin is *Serratia marcescens*, which is rod-shaped bacillus with gram-negative reaction belongs to the family Enterobacteriaceae [18].

This pigment has antibacterial activity against various bacteria, including *P. aeruginosa*. *Pseudomonas aeruginosa* may cause life-threatening wound infections due to its multidrug resistance and the presence of several pathogenicity factors during infections, whereas this bacterium is opportunistic non-spore forming, motile, rod-shaped and gram-negative aerobes. Different infections, such as the lung infection, skin infection and eyes of people with cystic fibrosis (CF), HIV/AIDS, and burns and abrasions, can caused by *P. aeruginosa*. These bacteria are ubiquitous microorganisms found in both natural and human-made environments, including those involving animals and plants [19-20].

MATERIALS AND METHODS

Collection, isolation and identification of bacteria

A total of one hundred-twenty samples of Pseudomonas aureginosa were obtained from burn and wound infections of different patients with several ages and include males and females 70 samples were collected from males and 50 from females, the ages ranged between 15-25, from two different hospitals namely, Al-Yarmouk, and Baghdad/Medical city during the period from December 2022 to February 2023. All samples were subjected to various examinations (cultural and biochemical examinations and VITEK2 system, antibiotic sensetivite (CLSI,2022) in order to isolate and identify isolates of *Pseudomonas aeruginosa*. In addition, forty samples were collected form soil for isolate *Serratia marcescens* with confirming its species using VITEK-2 system.and production of

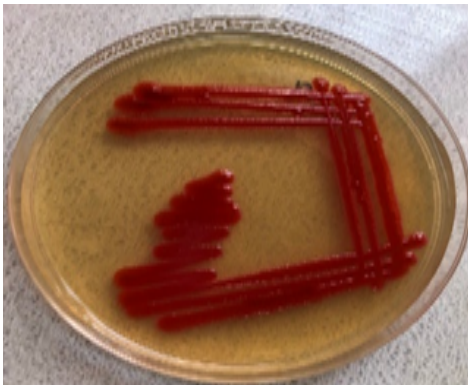

Fig. 1. *Serratia marcescens* on nutrient agar.

prodigiosin pigment test (Fig. 1).

Extraction and purification of Prodigiosin pigment

250 ml of S. marcescens was used to separate the raw prodigiosin. After 72 hours in culture, S. marcescens emerges as a gram-negative bacillus of the family Enterobacteriaceae in a cell-free broth culture. The centrifugation of the culture media at 8000 rpm for 15 minutes was performed. After removing the supernatant, 250 ml of methanol was added to the collected cells and they were vigorously mixed for 3 hours at room temperature. After centrifuging the resultant mixture for 20 minutes at 8000 rpm, the methanol filtrate was heated to 70 degrees Celsius in a rotary evaporator, and then chloroform was added at double the original volume in order to extract the red pigment. In a restorative funnel, the two solvents were blended well. The powder was made by collecting the chloroform phase (organic phase) and drying it at 45 C. Small amounts of water were used to dissolve the resultant pigment.

Synthesis of (iron) oxides nanoparticles

This was the first step in getting ready to biosynthesize Fe_2O_3 nanoparticles from the prodigiosin pigment. Nanoscale iron particles are those smaller than a micron in size. They're very reactive due to their enormous surface area. As soon as oxygen and water are introduced, they oxidise and release iron ions as a byproduct. They have found widespread use in medical and laboratory settings, and their potential for decontaminating industrial sites polluted with chlorinated organic compounds has been studied [17,18]. For the synthesis, 5mg of prodigiosin powder is mixed with 50ml of deionized distilled water DDW and sonicated for 30 minutes. Then, 5g of ferric sulphate is added to the mixture and the flask is shaken at room temperature in a darkroom

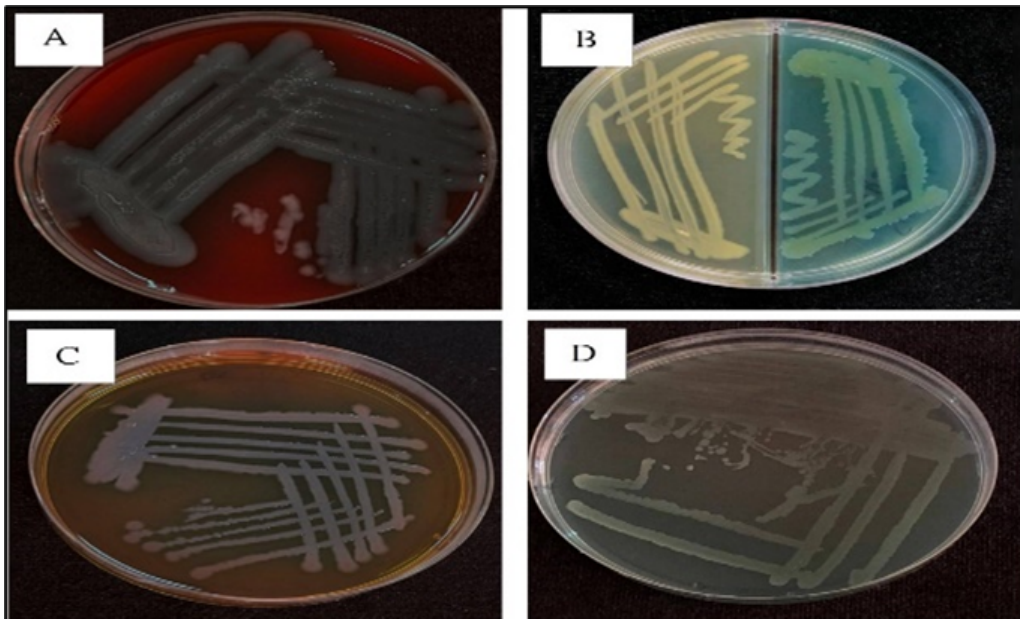

Fig. 2. Colonies of *P. aeruginosa* on: A) Blood agar, B) Cetrimide agar, C) MacConkey agar and D) *Pseudomonas* agar

Table 1. Biochemical test used in *P. aeruginosa* identification

Test	Result
Oxidase	+
Catalase	+
Indole test	-
Simmons Citrate test	+
Urease test	+

for an entire night. After that, we centrifuged the mixture at 5000 rpm for 10 minutes. Two washes with deionized water were used to flush out any leftover prodigiosin pigment from the precipitate of a solution containing entire iron oxides (Fe_2O_3) nanoparticles. Overnight, the nanoparticles that had precipitated were dried in an oven set to 40 degrees Celsius. Finally, a dark container was used to store the brown.

Synthesis of (iron and zinc) oxides core-shell nanoparticles (Fe_2O_3:ZnO)

used prodigiosin pigment for the biosynthesis of iron and zinc (**Fe_2O_3**:ZnO) core-shell nanoparticles, the Process iron oxides NP_S Which were previously prepared were used to synthesize

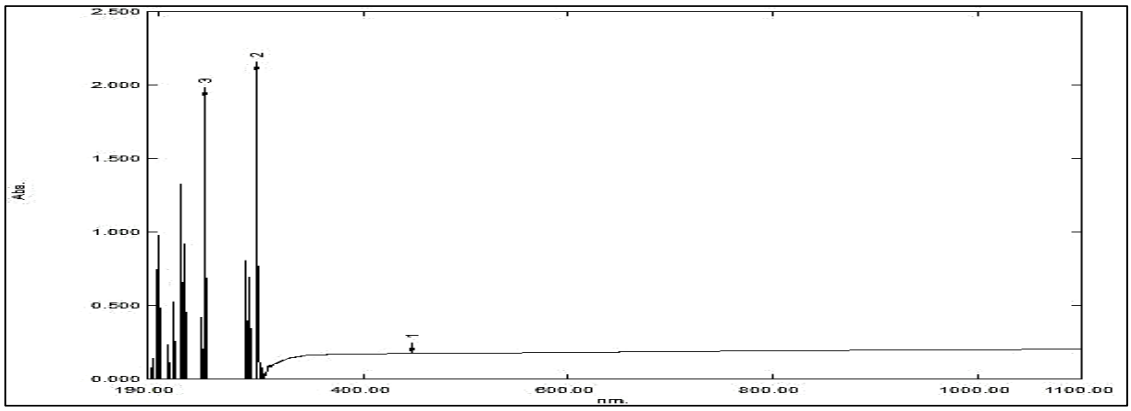

Fig. 3. UV-VIS of Fe_2O_3:ZnO core shell nanoparticles.

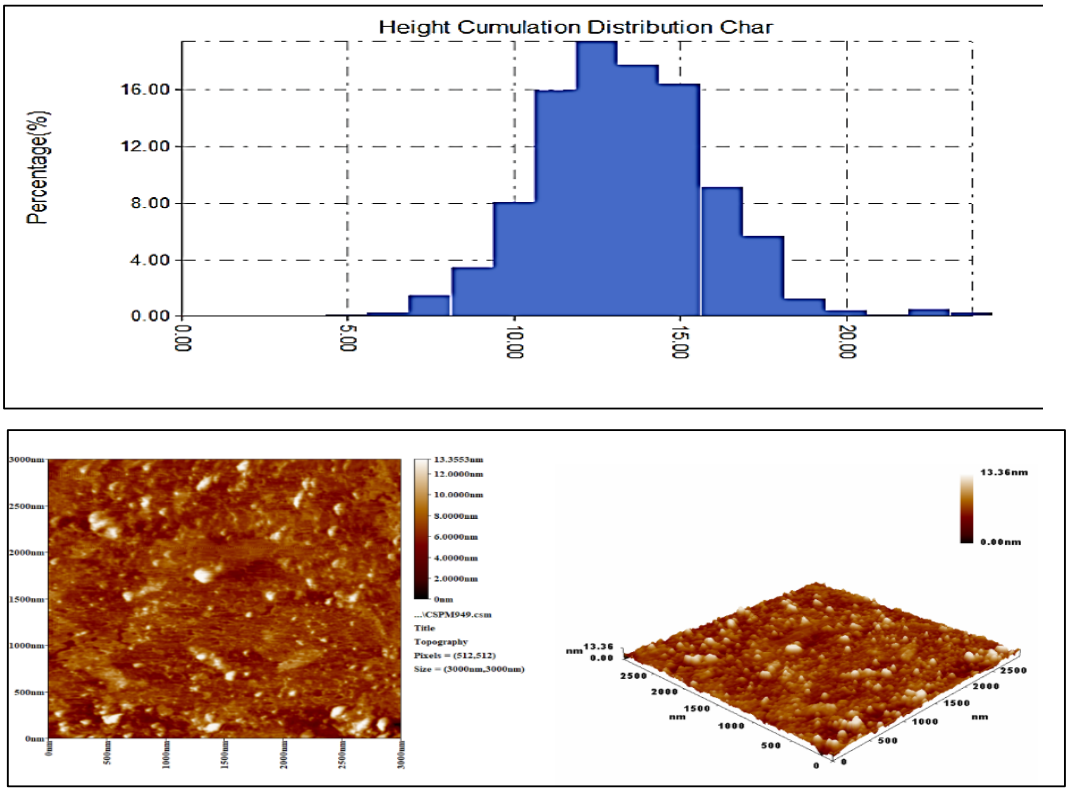

Fig. 4. Atomic Force Microscopy of iron oxide NPs (A: Histogram of iron oxide NPs, B: 2D and 3D of iron oxide nanoparticles).

iron and zinc (Fe_2O_3:ZnO) core-shell nanoparticles. The synthesis is carried out by dispersing 1.5 g of iron nanoparticles in 150 ml of prodigiosin pigment dispersed by ultrasonication bath for 30min using a magnetic stirrer plate. Add 5 g of zinc acetate into a flask and shake it overnight in a darkroom in room tempreuture . The mixture was then centrifuged for 10 minutes at 5000 rpm. The precipitate of a solution containing the whole iron and zinc (Fe_2O_3: ZnO) core-shell nanoparticles was twice washed with deionized distilled water to remove any remaining prodigiosin pigment. The precipitated nanoparticles were dried in an oven at 37°C overnight. Finally, the brown powder was sealed in a dark container to prevent it from evaporating [8].

Characterization of (Fe_2O_3:ZnO) oxides core-shell nanoparticles

Different techniques were utilized in order to characterize (Fe_2O_3: $ZnO_)$ including ultra-violate visible light (UV-Vis), atomic force microscopy (AFM), Fourier transforms infrared (FTIR) spectroscopy.

Estimation of antibacterial effect of Fe:ZnO_2 core-shell nanoparticles in comparison with Fe_2O_3 and ZnO nanoparticles separately

The agar well diffusion technique was used to determine the MIC of biologically generated Fe_2O_3, Zno or Fe_2O_3:ZnO NPs for their antibacterial properties against Gram-negative *P. aeruginosa*. 25 ml of sterile medium from Müller Hinton agar, solutions of varying concentrations of each nanoparticles (6.25,12.5, 25, 50,100 and 200 µg/ml) were introduced into the previously drilled wells. At 37 degrees Celsius, the obtained plates were infected for a period of 24 hours., it has been determined the size of the no-growth area surrounding each of the prepared wells.

RESULTS AND DISCUSSION

samples were collected from burn and wound infections a120sample from different patients with different ages and sexes, 70 samples were collected from males and 50 from females, the ages ranged between 15-25, during the period from December 2022 to February 2023. All samples were subjected

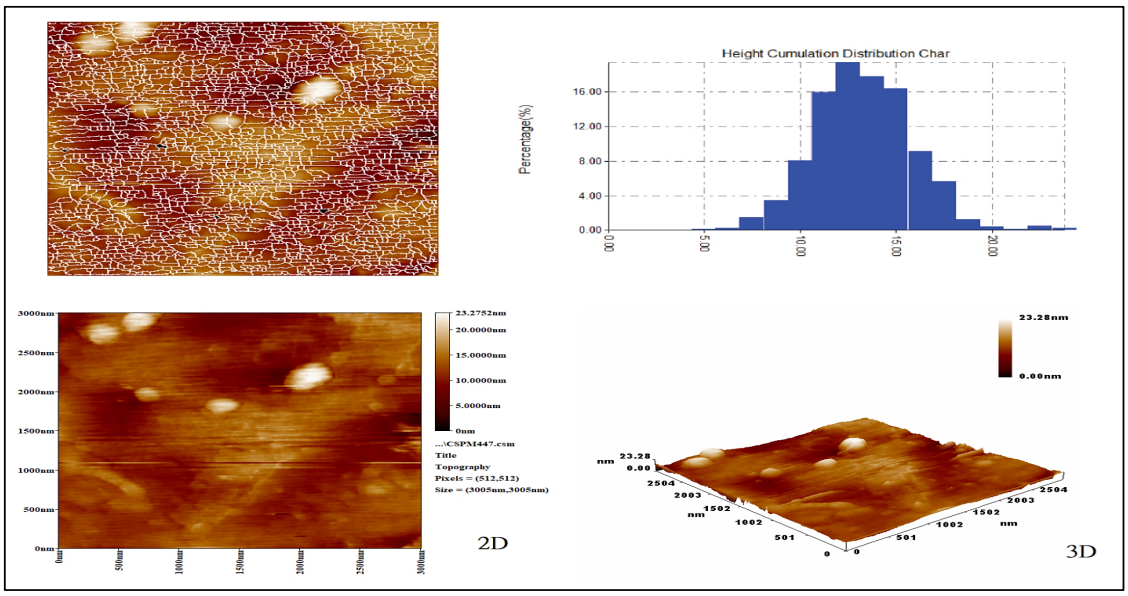

Fig. 5. Atomic force microscopy (AFM) of (Fe_2O_3:ZnO) nanoparticles synthesized using prodigiosin pigment.

Table 2. Average diameter of (Fe_2O_3:ZnO) nanoparticle.

Avg. Diameter:50.73 nm	<=10% Diameter:25.00 nm
<=50% Diameter:45.00 nm	<=90% Diameter:80.00 nm

to various examinations, with VITEK2 system, in order to isolate *Pseudomonas aeruginosa*.

Bacterial isolate based on analyses of morphological and, microscopic characteristics. Was subjected to several biochemical tests.

The performed by scanning a UV-visible spectrophotometer (Fig. 2) to detect the maximum absorption, the result showed the absorbance of Fe_2O_3:ZnO core shell nanoparticles at 320 nm. This result was identical to the result of the researcher (17,18) if the result was 287nm.

The surface shape formation of the Fe_2O_3 NPs was studied by atomic force microscopy to show that Fe_2O_3 NPs 2D and 3D. (Fig. 3). AFM images show that the synthesized Fe_2O_3 NPs are spherical. The size of an average diameter of 50.73nm was also measured by AFM Fig2**.** This result was identical to the result of the researcher (17,18).if the result was 35 nm

The surface shape formation of the (Fe_2O_3:ZnO) NPs was studied by atomic force microscopy to show that (Fe_2O_3:ZnO) NPs, (Fig. 2). AFM images show that the biosynthesized (Fe_2O_3:ZnO) NPS are spherical. The size of an average diameter of 81. 32 nm.We note that the size of the cor-shell is (81. 32) and the iron alone is (50.73). This increase in volume indicates the amount of zinc added to the iron. If the amount of zinc acetate was more, the packing zinc NPs would be more, and this was evident from their quantity in the EDX examination. Table 1.

The result of this measurement in the Fig. 5 and Table 3.

As can be seen in Fig. 3, the functional groups of nanoparticles have been identified using FTIR spectroscopy. Bands are seen in the FTIR absorption spectra of biologically synthesised nanoparticles at 3323.12–3284.55 cm^{-1}, which correspond to the stretching motion of hydroxyl groups in alcohols and hydroxyl bonds in phenols. The last peak is at 1629.74 cm-1 and is associated with the N-H bond in amines, whereas the peak at 1400.22-1095.49 cm^{-1} is caused by the O=bond in metal oxides.

Fe_2O_3:ZnO nanoparticles are spherical in shape, as seen by FE-SEM pictures; Despite the increased surface areas and surface energies of the Fe_2O_3 and ZnO core NPs, small amounts of agglomerates were observed on the surface of the nanoparticle film due to decreased surface energy and magnetic properties. The nanoparticles agglomerated due to the attractive physical interactions between them; this was made possible by the greater surface area to volume ratio. The shape of the prepared (Fe_2O_3:ZnO) nanoparticle was shown by FE- SEM analysis (Fig. 5).

A biological test using a device called a Vitek-2 compact system was used to determine whether of the bacterial isolates obtained were capable of producing prodigiosin. After 72 hours of incubation, manufacturing of prodigiosin began. At the conclusion of the exponential phase, the

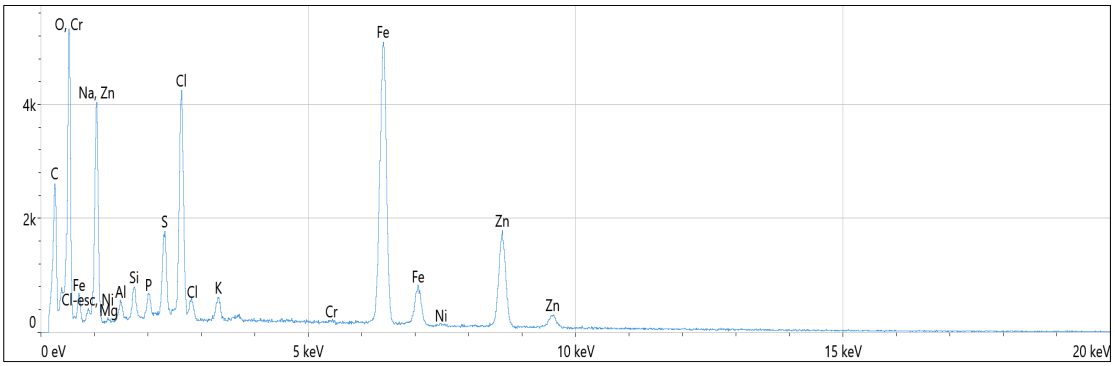

Fig. 6. Energy diffraction X- ray (EDX) of (Fe:ZnO) nanoparticles synthesized using prodigiosin.

Table 3. Average diameter of (Fe_2O_3:ZnO) nanoparticle.

Avg. Diameter:81.32 nm	<=10% Diameter:30.00 nm
<=50% Diameter:70.00 nm	<=90% Diameter:140.00 nm

concentration of prodigiosin in this study was 0.29 g/L after 48 hours of incubation, and 0.4145 g/L after 35 hours of incubation (during the stationary phase). The accumulation of prodigiosin, which occurred predominantly during the stationary phase, may account for the medium's reddish hue.

antibiotics were utilized in order to estimate the multi-drug resistance isolate of *P. aeruginosa*. These 10 antibiotics (symbol, µg) as follows: Tobramycin (TOB, 10 µg), Piperacillin-tazobactam

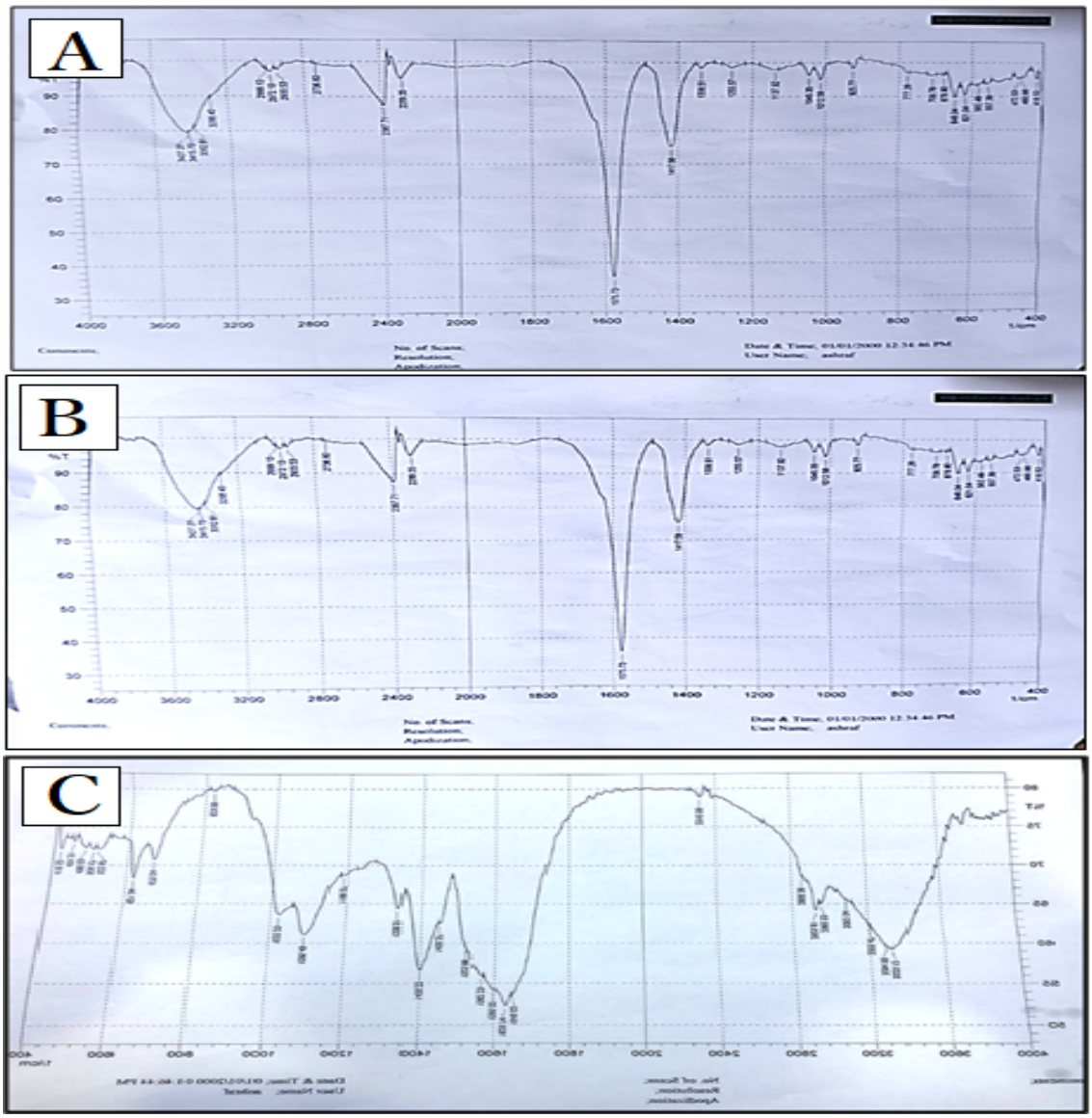

Fig. 7. FTIR images of (Fe_2O_3:ZnO) NPs synthesized using Prodigiosin pigment, A: Prodigiosin pigment. B Prodigiosin pigment + (Fe_2O_3:ZnO)NPs. C: (Fe_2O_3:ZnO) NPs.

Table 4. The data analysis of EDX

Element	Atomic%
5.9	Fe
3.0	Zn

(PIT, 100/10 µg), Meropenem (MEM, 10 µg), Azithromycin (AT, 30µg), Ceftazidime (CAZ, 30 µg), Piperacillin (PRL, 100 µg), Ofloxacin (OF, 5 µg), Levofloxacin (LE, 5 µg), Gentamicin (CN, 10 µg) and Imipenem (IPM, 10 µg) according to (CLSI.,2022), whereas the results were represented as resistance, intermediate and sensitive.

The antimicrobial activity of, iron oxide zinc oxideNPs and Fe_2O_3:ZnONPs core-shell against multi-drug resistant *Pseudomonas aeruginosa* were assessed. Varied concentrations of each utilized nanoparticles (6.25,12.5, 25, 50 ,100, and 200 µg/ml). Results of NPs antibacterial activity were demonstrated in (Fig. 6). The was found to be directly dependent upon the NPs concentrations. The maximum inhibition zone around *P. aeruginosa* isolate were (24, 18 and 27) mm at concentration 200 µg/ml of iron oxide NPs, zinc NPs and Fe:ZnO_2 core-shell NPs , whereas the minimum inhibition, zone was located at 25 µg/ml iron oxide (10)mm, whereas minimum inhibition, zone was located at 12.5 zinc oxide(7)mm and Fe:ZnO_2 core-shell NPs minimum inhibition, zone was located at concentrations 12.5 µg/ml. (8) mm,. The results demonstrated that there are significantly increase in antibacterial activity with increase of

Table 5. FTIR of (Fe_2O_3:ZnO) core shell nanoparticle.

Type of compound	Frequency of Absorption(cm^{-1}	bonds	Compound class of functional groups
Prodigiosin	3427.27-3415.91	O-H stretching	alcohol
	2387.71	S-H stretching	thiol
	1575.73	N-O stretching	nitro compound
	1417.58	S=O stretching	sulfate
Prodigiosin + (Fe2O3:ZnO) NPS	3454.27-3438.84	O-H stretching	alcohol
	1575.73	N-O stretching	nitro compound
	1427.23	O-H bending	carboxylic acid
	1108.99	C-O stretching	secondary alcohol
(Fe2O3:ZnO) NPs	3323.12 -3284.55	N-H stretching	Aliphatic primary amine
	2960.53-2925.81	C-H stretching	alkane
	1649.02-1629.74	C=C stretching	alkene
	1400.22	C-F stretching	fluoro compound
	1095.49	C-O stretching	secondary alcohol
	1022.49	C-N stretching	amine
	675.04	C-Br stretching	halo compound

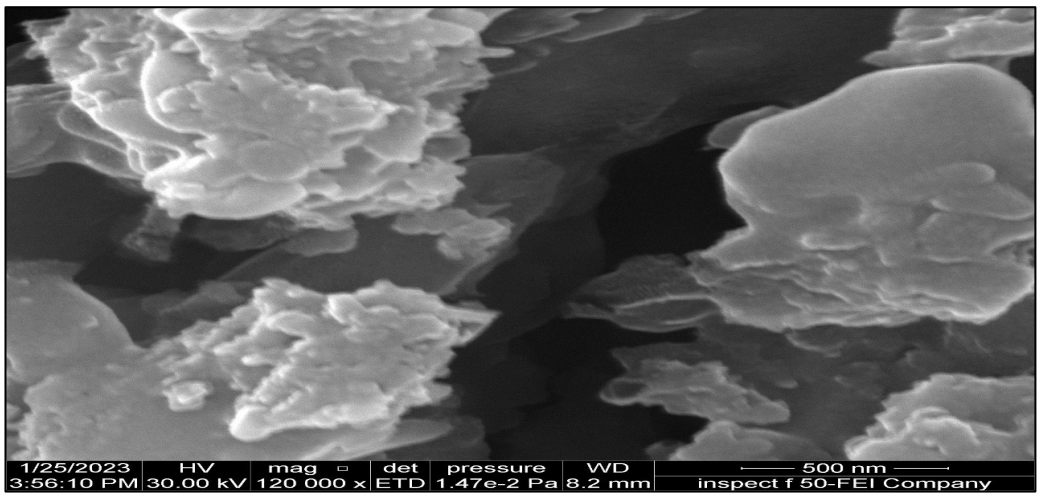

Fig. 8. FE-SEM images of Fe_2O_3:ZnO core-shell nanoparticles.

concentrations of each studied NPs as well as the core shell NPs shows better antimicrobial activity than each iron oxide and zinc oxide nanoparticles with respect to their concentrations, as shown in

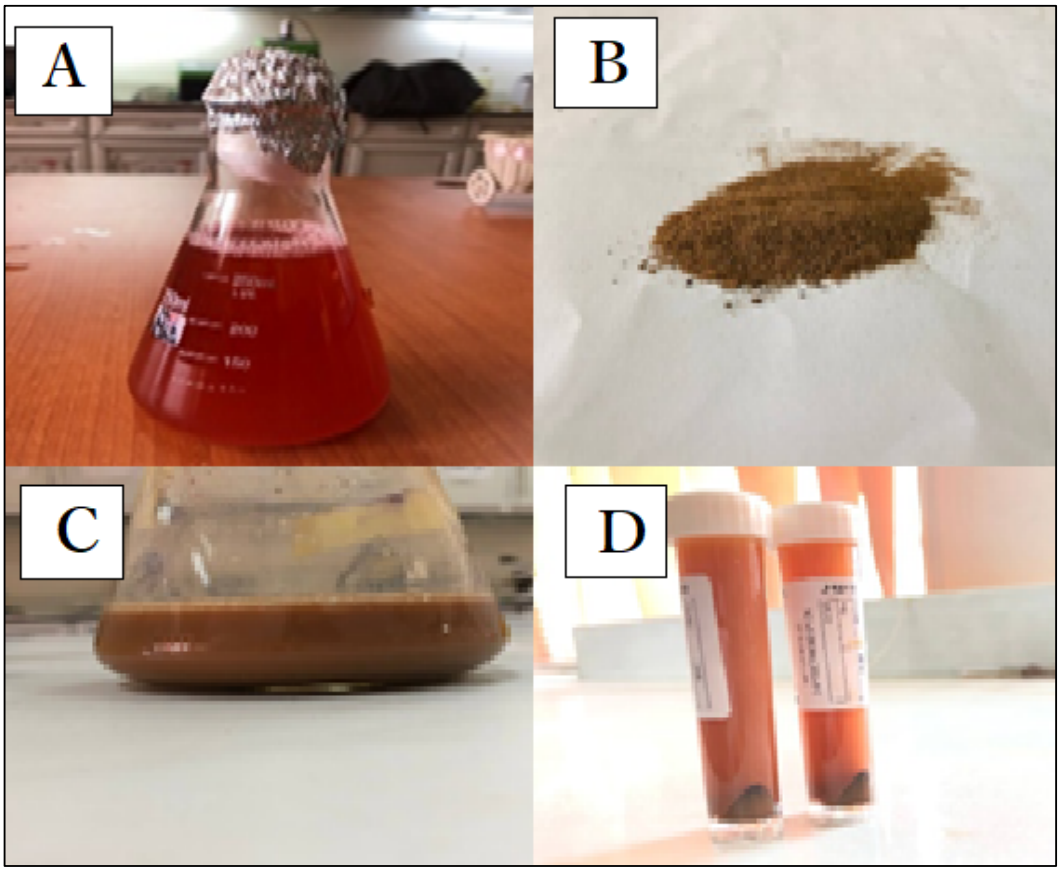

Fig. 9. A: Prodigiosin pigment after 72 hrs, B: Core-shell nanoparticles(Fe_2O_3:ZnO)powder, C: Core-shell nanoparticles(Fe_2O_3:ZnO),with Prodigiosin pigment D: Core-shell after centrifugation.

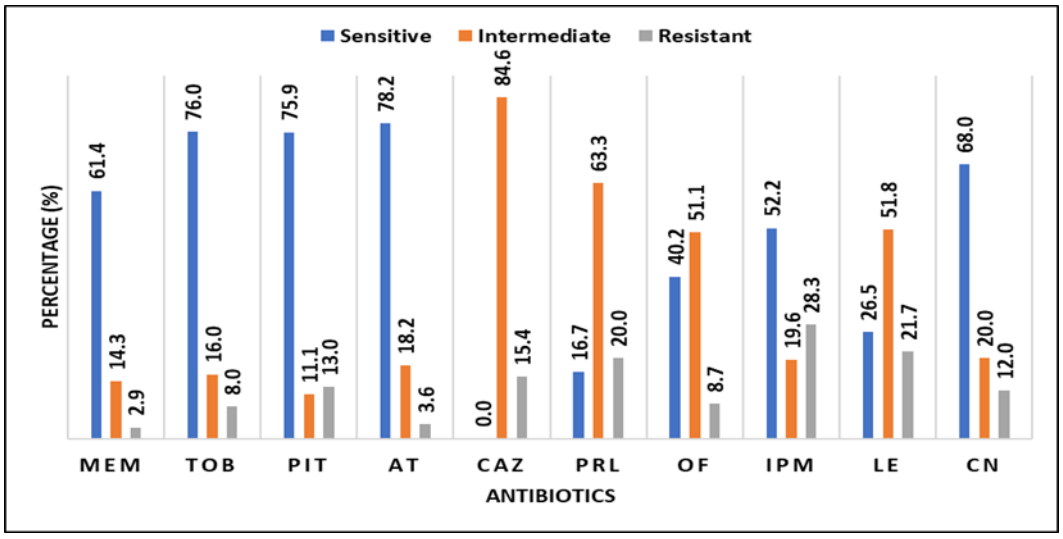

Fig. 10. The antibiotic susceptibility test.

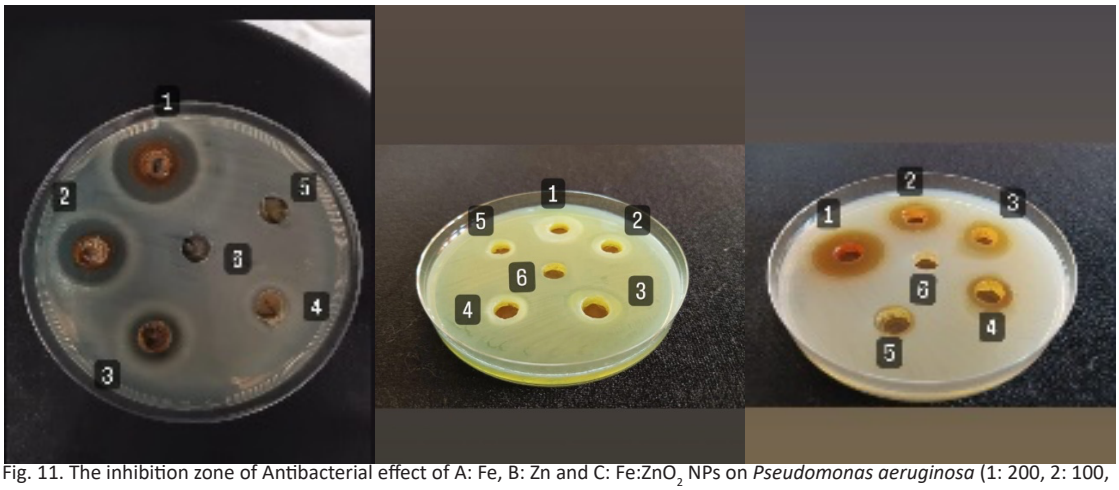

Fig. 11. The inhibition zone of Antibacterial effect of A: Fe, B: Zn and C: Fe:ZnO_2 NPs on *Pseudomonas aeruginosa* (1: 200, 2: 100, 3: 50, 4: 25, 5: 12.5 and 6: 6.25 µg/ml).

Table 6. The inhibition zone of Antibacterial effect of Fe, Zn and Fe_2O_3:ZnO NPs on *Pseudomonas aeruginosa*.

No.	Con.	Fe nanoparticles	Zn nanoparticles	Fe:ZnO_2 nanoparticles
	(µg/ml)	Zone of Diameter (mm)	Zone of Diameter (mm)	Zone of Diameter (mm)
1	200	24	18	27
2	100	20	16	23
3	50	15	13	17
4	25	10	9	14
5	12.5	No inhibition zone	7	8
6	6.25	No inhibition zone	No inhibition zone	No inhibition zone

Table 2.

Different interactions between NPs and the microorganism and the sensitivity of the bacteria employed in this investigation might account for the variation in the width of the inhibitory zones observed. Although microorganisms have negative charges, the positive charge of NPs associated with metal oxides causes electromagnetic interaction between the microorganisms and the metal oxides, resulting in oxidation and death. The capacity of harmful bacteria to enter the food chain of the environment makes the bactericidal activity of nanoparticles on bacteria of utmost relevance. Nanoparticles have been shown to have an antibacterial impact against bacteria and fungus, and this information is being communicated in current studies [17,18].

Hematite, or iron oxide, was found to be resistant to the acidity of the body and to kill bacteria through osmosis. Fenton's interaction between iron oxide nanoparticles and hydrogen peroxide in the cell's surroundings produces hydroxyl and peroxide free radicals in addition to reactive oxygen species. The production of reactive oxygen species (ROS) is the primary mechanism by which ZnO NPs exert their harmful effects on bacteria. In particular, the breakdown of biological components such proteins, lipids, and DNA contributes to ROS-induced toxicity to the cell membrane. The generation of ROS is widelyconsidered as the major factor of antibacterial activity associated with the ZnO phototoxicity. This in turn leads to oxidation which in turn kills/inhibits the microorganisms [2].

CONFLICT OF INTEREST

The authors declare that there is no conflict of interests regarding the publication of this

manuscript.

REFERENCES

1. Naji A, Ali K, Mohammad H, Alwan A. Serum hepcidin levels related to interlukin-6 in patients with acute myeloid leukemia before and after treatment. Iraqi Journal of Hematology. 2022;11(1):76.
2. Alaa Alden MA, Yaaqoob LA. Evaluation of the biological effect synthesized zinc oxide nanoparticles on pseudomonas aeruginosa. iraqi journal of agricultural sciences. 2022;53(1):27-37.
3. Al-Hasnawy H. Sequence Analysis of Novel Genes in Clinical and Environmental Pseudomonas aeruginosa Iraqi Isolates. Journal of Pure and Applied Microbiology. 2018;12(1):29-40.
4. Bhushan M, Mohapatra D, Kumar Y, Kasi Viswanath A. Fabrication of novel bioceramic α-Fe_2O_3/MnO nanocomposites: Study of their structural, magnetic, biocompatibility and antibacterial properties. Materials Science and Engineering: B. 2021;268:115119.
5. Brokesh AM, Gaharwar AK. Inorganic Biomaterials for Regenerative Medicine. ACS Applied Materials & Interfaces. 2020;12(5):5319-5344.
6. Gohil N, Bhattacharjee G, Singh V. Synergistic bactericidal profiling of prodigiosin extracted from Serratia marcescens in combination with antibiotics against pathogenic bacteria. Microb Pathog. 2020;149:104508.
7. Guo Z, Chen Y, Wang Y, Jiang H, Wang X. Advances and challenges in metallic nanomaterial synthesis and antibacterial applications. Journal of Materials Chemistry B. 2020;8(22):4764-4777.
8. Sarah FA-T, Dhafar NA-U, Khawla AK, Laith AY. Antibacterial effects of Ceftriaxone/Zinc Oxide Nanoparticles Combination Against Ceftriaxone resistant Escherichia coli isolated from Urinary Tract Infections. Indian Journal of Forensic Medicine & Toxicology. 2021;16(1):1080-1088.
9. Hussein K. Detection of the antimicrobial activity of silver nanoparticules biosynthesized by streptococcus pyogenes bacteria. Iraqi Journal of Agricultural Sciences. 2020;51(2):500-507.
10. Jayaprakashvel M, Sami M, Subramani R. Antibiofilm, Antifouling, and Anticorrosive Biomaterials and Nanomaterials for Marine Applications. Nanotechnology in the Life Sciences: Springer International Publishing; 2020. p. 233-272.
11. Lyngsie G, Krumina L, Tunlid A, Persson P. Generation of hydroxyl radicals from reactions between a dimethoxyhydroquinone and iron oxide nanoparticles. Sci Rep. 2018;8(1).
12. Morens DM, Folkers GK, Fauci AS. Emerging infections: a perpetual challenge. The Lancet Infectious Diseases. 2008;8(11):710-719.
13. Prabhu D, Rajamanikandan S, Anusha SB, Chowdary MS, Veerapandiyan M, Jeyakanthan J. In silico Functional Annotation and Characterization of Hypothetical Proteins from Serratia marcescens FGI94. Biol Bull. 2020;47(4):319-331.
14. Rudra B, Gupta RS. Phylogenomic and comparative genomic analyses of species of the family Pseudomonadaceae: Proposals for the genera Halopseudomonas gen. nov. and Atopomonas gen. nov., merger of the genus Oblitimonas with the genus Thiopseudomonas, and transfer of some misclassified species of the genus Pseudomonas into other genera. International Journal of Systematic and Evolutionary Microbiology. 2021;71(9).
15. Wood SJ, Kuzel TM, Shafikhani SH. Pseudomonas aeruginosa: Infections, Animal Modeling, and Therapeutics. Cells. 2023;12(1):199.
16. Xu W, Qing X, Liu S, Chen Z, Zhang Y. Manganese oxide nanomaterials for bacterial infection detection and therapy. Journal of Materials Chemistry B. 2022;10(9):1343-1358.
17. Kamel RM, Yaaqoob LA. Evaluation of the biological effect synthesized iron oxide nanoparticles on enterococcus faecalis. iraqi journal of agricultural sciences. 2022;53(2):440-452.
18. Ali Z, Risan MH. Green synthesis of zinc oxide nanoparticles and its antibacterial Activity on Pseudomonas aeruginosa. Journal of Biotechnology Research Center. 2024;18(2):5-16.
19. Yaseen Rashid H, Mohammed Ali AS, Mohammed AI. Effect of calcination temperature on the adsorption performance of mg/al layered double hydroxide nanoparticles in the removal of meropenem antibiotics. Iraqi Journal of Agricultural Sciences. 2023;54(1):42-58.
20. younis rw. production, purification and inhibition of alginate ly-ase from local isolate of pseudomonas aeruginosa na11. iraqi journal of agricultural sciences. 2020;51(6):1726-1739.